Space charge and screening of a supercritical impurity cluster in monolayer graphene

Eugene B. Kolomeisky ●[1] and Joseph P. Straley[2]

[1]*Department of Physics, University of Virginia, P. O. Box 400714, Charlottesville, Virginia 22904-4714, USA*
[2]*Department of Physics and Astronomy, University of Kentucky, Lexington, Kentucky 40506-0055, USA*

A Coulomb impurity of charge Ze is known to destabilize the ground state of undoped graphene with respect to creation of screening space charge when Z exceeds the critical value $Z_c = 1/2\alpha$ set by the material's fine structure constant α. Recent experimental advances have made it possible to explore this transition in a controlled manner by tuning Z across the critical point. Combined with relatively large value of α this makes it possible to study graphene's screening response to a supercritical impurity $Z\alpha \gg 1$ when the screening charge is large using a Thomas-Fermi analysis. The character of screening in this regime is controlled by the dimensionless screening parameter $Z\alpha^2$. Specifically, for a circular impurity cluster in the weak-screening regime $Z\alpha^2 \ll 1$ most of the screening charge is found to reside outside the cluster. The strong-screening regime $Z\alpha^2 \gg 1$ provides a realization of the Thomson atom: Most of the screening charge is inside the cluster, nearly perfectly neutralizing the source charge with the exception of a transition layer near the cluster's edge where the rest of the space charge is localized.

I. INTRODUCTION

Monolayer graphene is a two-dimensional semimetal whose low-energy elementary excitations obey a pseudorelativistic dispersion law

$$\varepsilon(\mathbf{p}) = \pm v_F p, \qquad (1)$$

where $\mathbf{p}$ is the two-dimensional momentum vector, $p = |\mathbf{p}|$, the upper and lower signs correspond to the conduction and valence bands, respectively, and $v_F \approx c/300$ is the Fermi velocity [1].

This paper studies the screening response of undoped pristine graphene to a large external impurity charge Ze (which we may assume to be positive without the loss of generality). Fundamental interest in this problem can be quickly appreciated by trying to understand the binding properties of the Coulomb field. Indeed, the ground-state energy of graphene's electron of typical momentum p localized within a spatial scale $r \simeq \hbar/p$ can be estimated by optimizing the energy cost of localization according to Eq. (1) against the potential energy gain in the electric field of charge Ze,

$$\varepsilon(p) \simeq v_F p - \frac{Ze^2}{\kappa r} \simeq v_F p(1 - Z\alpha), \quad \alpha = \frac{e^2}{\kappa \hbar v_F} \approx \frac{2.5}{\kappa}, \qquad (2)$$

where κ is the dielectric constant due to graphene's own electrons and the surrounding environment, and α is the material's fine structure constant [1]. Minimizing with respect to the parameter p one can then see that when the dimensionless external charge Z (hereafter simply referred to as "charge") is sufficiently small, $Z\alpha \lesssim 1$, the electron is delocalized, $p \propto 1/r = 0$, while sufficiently large charge, $Z\alpha \gtrsim 1$, leads to an infinitely sharp localization $p \propto 1/r = \infty$.

Essentially, the same conclusion applies to the charge state of a point nucleus of charge Ze in vacuum, where now the fine structure constant $\alpha = e^2/\hbar c = 1/137$ is significantly smaller: The electric field of a highly charged nucleus ($Z \gtrsim 137$) destabilizes the vacuum with respect to creation of electron-positron pairs; the positrons escape to infinity leaving behind a screening space charge of electrons [2]. Creating a charge exceeding $137e$ is a serious obstacle to experimental observation of the vacuum instability, but for the suspended graphene the predicted threshold value $Z_c = 1/2\alpha \approx \kappa/5$ [3] is experimentally accessible, since $\kappa \approx 5$ and thus, $\alpha \approx 1/2$ [4]), resulting in $Z_c \approx 1$.

Various aspects of atomic collapse in graphene have been verified in experiments with clusters of charged Ca dimers [5]. More recently a tunable version of the external charge Z was realized [6]: A single-atom vacancy in graphene was demonstrated to stably host a local charge and this charge could be gradually built up by applying small voltage pulses with the tip of a scanning tunneling microscope (STM). The experiment has been performed using a variety of surfaces, specifically, G/G/BN [graphene (G) on graphene on Boron nitride (BN)], G/BN and G/G on SiO_2, and each sample was independently characterized regarding its value of the parameter α (1). This allowed to systematically study a range of charges both below and above $Z_c = 1/2\alpha$, up to $Z \approx 1.6/\alpha$ (G/G/BN surface). When Z exceeds Z_c but is still close to it, there are very few screening electrons present, and one faces a difficult few-body problem of the binding of graphene's electrons to a Coulomb center. A simplification arises in the many-electron case ($Z \gg 1$) when the Thomas-Fermi (TF) method applies [7]. Its main advantages are physical transparency and rigor: Correlation effects vanish to leading order as $Z \to \infty$ so that a mean-field treatment of electron-electron interactions suffices [8]. Here we revisit the TF theory for a supercritical $Z\alpha \gg 1$ impurity cluster in graphene. This regime also appears to be within experimental reach of the approach of Ref. [6]; it seems plausible that a large charge corresponding to $Z\alpha \gg 1$ can be built up by applying voltage

pulses with the STM tip to individual vacancies of a vacancy cluster.

The TF theory in question has been analyzed by several authors [9–11] with conflicting predictions which were attributed to physically different regimes of parameter values [11]. A comprehensive physical picture of the effect, including analysis of the geometry relevant to the most promising experimental setup [6] is, in our judgment, still lacking. Our contribution below brings completeness and definiteness to the problem of screening of a $Z\alpha \gg 1$ impurity in graphene. Our analysis builds on a study due to Migdal *et al.* [12] of the QED version of the related problem that was adopted [13] to the case of narrow band-gap semiconductors [14] and Weyl semimetals [15]. The latter systems may be viewed as three-dimensional counterparts of graphene, and below we indeed find that the physics of supercritical impurity screening in graphene resembles that of a Weyl semimetal [13]. The difference between the problems is largely technical and traceable to two-dimensionality of graphene's electrons interacting according to the three-dimensional Coulomb law.

We hasten to mention that the approach of Refs. [12,13] has been also employed to solve the problem of the collapse of the electrons to a donor cluster in SrTiO$_3$ [16].

II. CLASSICAL ELECTROSTATICS

The total electrostatic potential $\varphi(\mathbf{r})$ felt by an electron confined to a plane embedded into three-dimensional space is due to an external potential $\varphi_{\text{ext}}(\mathbf{r})$ and to the potential caused by the rest of the screening electron cloud of number density $n(\mathbf{r})$:

$$
\begin{aligned}
\varphi(\mathbf{r}) &= \varphi_{\text{ext}}(\mathbf{r}) - \frac{e}{\kappa} \int \frac{n(\mathbf{r}')d^2r'}{|\mathbf{r}-\mathbf{r}'|} \\
&= \frac{1}{\kappa} \int \frac{\sigma(\mathbf{r}')d^2r'}{|\mathbf{r}-\mathbf{r}'|} = \frac{e}{\kappa} \int \frac{[n_{\text{ext}}(\mathbf{r}')-n(\mathbf{r}')]d^2r'}{|\mathbf{r}-\mathbf{r}'|}, \quad (3)
\end{aligned}
$$

where $\mathbf{r}$ is the two-dimensional position vector, $\sigma(\mathbf{r}) = e[n_{\text{ext}}(\mathbf{r}) - n(\mathbf{r})]$ is the surface charge density, and an external number density $n_{\text{ext}}(\mathbf{r})$ is related to $\varphi_{\text{ext}}(\mathbf{r})$ as

$$
\varphi_{\text{ext}}(\mathbf{r}) = \frac{e}{\kappa} \int \frac{n_{\text{ext}}(\mathbf{r}')d^2r'}{|\mathbf{r}-\mathbf{r}'|}. \quad (4)
$$

The integrals are over the plane where the charge resides, but the Coulomb interaction has a three-dimensional form since the fields extend into space. We note that external charges positioned off the plane also create in-plane φ_{ext}; in such cases Eq. (4) defines an equivalent in-plane n_{ext}. Given φ_{ext}, Eq. (4) can be inverted to provide an explicit expression for n_{ext}. In a compact form this can be given in terms of the Fourier transforms of the potential, $\varphi_{\text{ext}}(\mathbf{q})$, and the density

$$
n_{\text{ext}}(\mathbf{q}) = \frac{\kappa}{2\pi e} q \varphi_{\text{ext}}(\mathbf{q}), \quad (5)
$$

where $q = |\mathbf{q}|$. For the external potential of charge Z one has $\varphi_{\text{ext}}(\mathbf{q} \to 0) = 2\pi Ze/\kappa q$, thus implying that $n_{\text{ext}}(\mathbf{q} \to 0) = Z$ which is a restatement that we are dealing with net charge Z. For example, for a point charge Z that is a distance

a away from the plane, the external in-plane potential is

$$
\varphi_{\text{ext}}(\mathbf{r}) = \frac{Ze}{\kappa(r^2+a^2)^{1/2}}. \quad (6)
$$

Then $\varphi_{\text{ext}}(\mathbf{q}) = (2\pi Ze/\kappa q)e^{-qa}$ and, following Eq. (5) z one finds $n_{\text{ext}}(\mathbf{q}) = Ze^{-qa}$. Inverting the Fourier transform gives the real-space density

$$
n_{\text{ext}}(\mathbf{r}) = \frac{Za}{2\pi(r^2+a^2)^{3/2}}. \quad (7)
$$

As another example, let us consider in-plane charge distribution that is Gaussian in the Fourier representation, $n_{\text{ext}}(\mathbf{q}) = Ze^{-q^2a^2}$. Then it is also Gaussian in real space:

$$
n_{\text{ext}}(\mathbf{r}) = \frac{Z}{4\pi a^2} e^{-r^2/4a^2}. \quad (8)
$$

Following Eq. (5), the external potential is $\varphi_{\text{ext}}(\mathbf{q}) = (2\pi Ze/\kappa q)e^{-q^2a^2}$ whose inversion [17] supplies its real-space version

$$
\varphi_{\text{ext}}(\mathbf{r}) = \frac{\sqrt{\pi}}{2} \frac{Ze}{\kappa a} e^{-r^2/8a^2} I_0\left(\frac{r^2}{8a^2}\right), \quad (9)
$$

where $I_0(y)$ is a modified Bessel function of the first kind.

Equation (3) makes it clear that the regime of infinitesimally weak screening is

$$
\varphi(\mathbf{r}) = \varphi_{\text{ext}}(\mathbf{r}), \quad n(\mathbf{r}) = 0, \quad (10)
$$

while the regime of infinitely strong screening is

$$
\varphi(\mathbf{r}) = 0, \quad n(\mathbf{r}) = n_{\text{ext}}(\mathbf{r}). \quad (11)
$$

For example, for point charge Z positioned a distance a away from the ideally conducting (i.e., screening) plane, $n = n_{\text{ext}}$ given by Eq. (7) is the textbook result for the density of induced charge derived by the method of images.

When the source has circular symmetry, angular integration can be carried out in Eq. (3) with the result

$$
\varphi(r) = \frac{4}{\kappa r}\int_0^r \sigma(r')r'dr'\mathbf{K}\left(\frac{r'}{r}\right) + \frac{4}{\kappa}\int_r^\infty \sigma(r')dr'\mathbf{K}\left(\frac{r}{r'}\right), \quad (12)
$$

where $\mathbf{K}(y)$ is the complete elliptic integral of the first kind and we employed Landen's transformation [17]. On the other hand, electrostatic potential of a three-dimensional spherically symmetric charge density distribution $\rho(r)$ can be written as

$$
\varphi(r) = \frac{4\pi}{\kappa r}\int_0^r \rho(r')r'^2dr' + \frac{4\pi}{\kappa}\int_r^\infty \rho(r')r'dr'. \quad (13)
$$

Comparing Eq. (12) with its three-dimensional counterpart (13) highlights the mathematical difference between screening problems in two and three dimensions. Indeed, multiplying both sides of (13) by r and twice differentiating the outcome, one recovers the Poisson's equation $\partial^2(r\varphi)/r\partial r^2 = -4\pi\rho/\kappa$. Similar exact reduction to a differential form is impossible with Eq. (12), thus leaving us with a singular integral equation. Nevertheless, a useful simplification of Eq. (12) capturing the physics of the problem is possible, and based on the observation that $\mathbf{K}(y)$ is nearly constant and slightly exceeds $\pi/2$ over most of its range with the exception of the narrow vicinity of $y = 1$ where it has integrable (logarithmic)
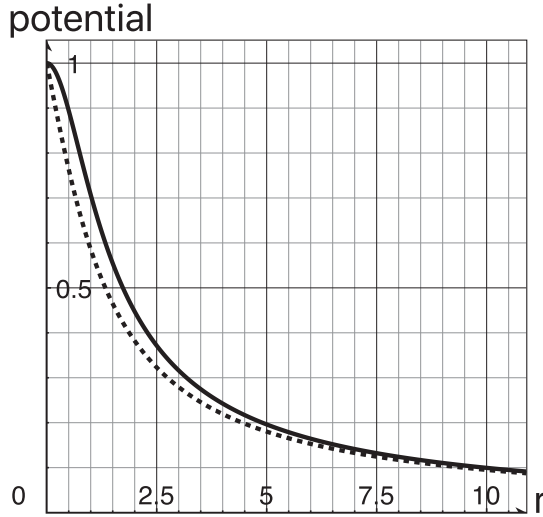
potential

FIG. 1. In-plane electrostatic potential (in units of $Ze/\kappa a$) versus distance (in units of a) due to a point charge outside the conductive plane: Exact result (6) (bold curve) versus its approximation (15) (dashed curve).

singularity. Then, approximating $\mathbf{K}(y) \rightarrow \mathbf{K}(0) = \pi/2$ in the integrands in Eq. (12) reduces the latter to the form

$$\varphi(r) \approx \frac{2\pi}{\kappa r}\int_0^r \sigma(r')r'dr' + \frac{2\pi}{\kappa}\int_r^\infty \sigma(r')dr', \quad (14)$$

which matches the exact result (12) both for $r \rightarrow 0$ and $r \rightarrow \infty$. To illustrate its accuracy for general r, we computed the approximate potential (14) corresponding to the density (7) with the result

$$\varphi_{\text{ext}}^{(\text{appr})}(r) = \frac{Ze}{\kappa a}\frac{r + a - \sqrt{r^2 + a^2}}{r}. \quad (15)$$

Its comparison with the exact potential (6) displayed in Fig. 1 shows that Eq. (14) is a good approximation to Eq. (12) for all r.

Multiplying both sides of Eq. (14) by r and twice differentiating the outcome, one obtains equivalent differential equation

$$\frac{\partial^2(r\varphi)}{\partial r^2} \approx -\frac{2\pi\sigma}{\kappa} = -\frac{2\pi e}{\kappa}(n_{\text{ext}} - n). \quad (16)$$

Its consequence is that the total charge within a circle of radius r is approximately given by

$$\mathcal{Z}(r) \approx -\frac{\kappa}{e}r^2\frac{\partial\varphi}{\partial r}. \quad (17)$$

Introducing a screening function $\zeta(r)$ according to

$$\varphi = \frac{\zeta(r)e}{\kappa r}, \quad (18)$$

the charge (17) can be written as

$$\mathcal{Z}(r = Re^l) = \zeta(l) - \zeta'(l), \quad (19)$$

where R is an arbitrary length scale. We see that for $l \gg 1$ (r large) when the first derivative term $\zeta'(l)$ is negligible compared to $\zeta(l)$, the distinction between the screening function and the charge disappears, i.e., $\mathcal{Z} \approx \zeta$.

III. THOMAS-FERMI THEORY

In order to understand what determines the strength of screening in graphene and to go beyond the limiting cases (10) and (11), classical electrostatics accumulated in Eqs. (3)–(5) has to be supplemented by relevant information about the physics of pristine graphene. In the TF theory this is contained in the statement that $e\varphi$ causes a local change in the chemical potential, such as in thermodynamic equilibrium, the electrochemical potential remains zero across the system (the effect of finite doping has been considered in Ref. [10]),

$$\mu = \mu_0(n) - e\varphi(\mathbf{r}) = \hbar v_F\sqrt{\pi n} - e\varphi(\mathbf{r}) = 0. \quad (20)$$

Here $\mu_0(n) = \hbar v_F\sqrt{\pi n}$ is the chemical potential of graphene's electrons in the absence of a perturbing potential $\varphi(\mathbf{r})$ [1], and the density n is assumed to be small enough so that the dispersion law (1) applies. Equation (20) implies a relationship between the density n and total potential φ

$$n = \frac{1}{\pi}\left(\frac{e\varphi}{\hbar v_F}\right)^2. \quad (21)$$

For the external potential of charge Z one expects either partial or complete screening, i.e., $\varphi(r \rightarrow \infty) = \mathcal{Z}(\infty)e/\kappa r$, where $0 \leqslant \mathcal{Z}(\infty) < Z$ is observable charge at large distance from the source. Taking the $r \rightarrow \infty$ limit in the first representation in Eq. (3), one naturally finds $\mathcal{Z}(\infty) = Z - \int n(\mathbf{r})d^2r$ which is consistent with Eq. (21) only if $\mathcal{Z}(\infty) = 0$. Otherwise, the density, according to Eq. (21), falls off as $1/r^2$ which is not normalizable. Therefore, the screening is complete, $\int n(\mathbf{r})d^2r = Z$, with the potential and density falling off at r large faster than $1/r$ and $1/r^2$, respectively.

Combing Eq. (21) with the first representation for φ in Eq. (3) leads to the nonlinear integral TF equation [10,11]:

$$\varphi(\mathbf{r}) = \varphi_{\text{ext}}(\mathbf{r}) - \frac{e}{\pi\kappa}\left(\frac{e}{\hbar v_F}\right)^2\int\frac{\varphi^2(\mathbf{r}')d^2r'}{|\mathbf{r} - \mathbf{r}'|}. \quad (22)$$

An equivalent equation can be given in terms of the density by substituting (21) into the second representation in Eq. (3) and employing the relationship (4),

$$\sqrt{n(\mathbf{r})} = \frac{\alpha}{\sqrt{\pi}}\int\frac{[n_{\text{ext}}(\mathbf{r}') - n(\mathbf{r}')]d^2r'}{|\mathbf{r} - \mathbf{r}'|}. \quad (23)$$

The same equation can be obtained by minimization of the TF energy functional

$$E[n] = \frac{2\sqrt{\pi}}{3}\hbar v_F\int n^{3/2}(\mathbf{r})d^2r - e\int\varphi_{\text{ext}}(\mathbf{r})n(\mathbf{r})d^2r$$
$$+ \frac{e^2}{2\kappa}\int\frac{n(\mathbf{r})n(\mathbf{r}')d^2rd^2r'}{|\mathbf{r} - \mathbf{r}'|}, \quad (24)$$

where the first term represents quantum-mechanical effect of the zero-point motion—it is the kinetic energy of the screening cloud—while the rest encompasses classical electrostatics.

Below we assume that the external potential is circularly symmetric and due to charge Z localized within a region of typical size a:

$$\varphi_{\text{ext}}(\mathbf{r}) = \frac{Ze}{\kappa a}f_{\text{ext}}\left(\frac{r}{a}\right), \quad f_{\text{ext}}(x \rightarrow \infty) = \frac{1}{x}, \quad (25)$$

where $f_{\text{ext}}(x = 0)$ is finite. Measuring the length in units of a, potential in units of $Ze/\kappa a$, and density in units of Z/a^2 prompts introduction of dimensionless counterparts of the potential ($\varphi \to f$), density ($n \to \nu$), and external density ($n_{\text{ext}} \to \nu_{\text{ext}}$); the latter two are now normalized at unity. In terms of these new functions and scales, Eqs. (21)–(23) acquire the form

$$\nu = \gamma f^2, \quad \gamma = \frac{Z\alpha^2}{\pi}, \tag{26}$$

$$f(x) = f_{\text{ext}}(x) - \gamma \int \frac{f^2(x')d^2x'}{|\mathbf{x} - \mathbf{x}'|}, \tag{27}$$

$$\sqrt{\nu(x)} = \sqrt{\gamma} \int \frac{[\nu_{\text{ext}}(x') - \nu(x')]d^2x'}{|\mathbf{x} - \mathbf{x}'|}. \tag{28}$$

The solution of the problem is thus determined by the shape of the external charge distribution and single dimensionless parameter $\gamma \simeq Z\alpha^2$ which controls the strength of screening [11]. Indeed, taking the infinitesimally weak screening limit $\gamma \to 0$ in Eqs. (26) and (27) recovers Eq. (10), while taking the infinitely strong screening limit $\gamma \to \infty$ in Eqs. (26) and (28) derives Eq. (11).

It is also useful to rewrite the energy functional (24) in terms of the dimensionless density $\nu(x)$ and the external potential $f_{\text{ext}}(x)$,

$$E[\nu] = \frac{Z^2 e^2}{\kappa a} \left\{ \frac{2}{3\sqrt{\gamma}} \int \nu^{3/2}(x)d^2x - \int f_{\text{ext}}(x)\nu(x)d^2x \right.$$
$$\left. + \frac{1}{2} \int \frac{\nu(x)\nu(x')d^2x d^2x'}{|\mathbf{x} - \mathbf{x}'|} \right\}, \tag{29}$$

which additionally demonstrates that the limit of infinitely strong screening $\gamma \to \infty$ is classical while quantum effects dominate interactions in the regime of infinitesimally weak screening $\gamma \to 0$. This equation shows natural scaling of the energy with Z, e, κ, and a, and explains why the problem is ill defined in the point charge limit $a = 0$. The fact that the external charge must be spread over finite-sized region imposes practical limitation on how large Z can be for given a. We assume that appropriate conditions discussed in Ref. [11] are met.

In the circularly symmetric case of interest (25), the integral Eq. (22) transforms into

$$\varphi(r) = \varphi_{\text{ext}}(r) - \frac{4e}{\pi \kappa r} \left(\frac{e}{\hbar v_F}\right)^2 \int_0^r \varphi^2(r')r'dr'\mathbf{K}\left(\frac{r'}{r}\right)$$
$$- \frac{4e}{\pi \kappa} \left(\frac{e}{\hbar v_F}\right)^2 \int_r^\infty \varphi^2(r')dr'\mathbf{K}\left(\frac{r}{r'}\right) \tag{30}$$

and corresponding versions of Eqs. (23), (24), and (27)–(29) can be similarly given.

In assessing the range of applicability of the TF theory we first observe that it overlooks the atomic collapse effect discussed in the introduction. Indeed, according to Eq. (21), arbitrarily small potential induces space charge (because the energy gap is zero) while from the single-particle standpoint there is a screening threshold at $Z_c = 1/2\alpha$. The resolution [3,11], like in the problem of impurity screening in Weyl semimetal [13], is that the prediction of complete screening

$\mathcal{Z}(\infty) = 0$, the exact property of the TF theory, is an artifact; the observable charge for $Z \geqslant Z_c = 1/2\alpha$ is the critical charge $\mathcal{Z}(\infty) = 1/2\alpha$. This means that our analysis holds provided $\mathcal{Z}(r) \gg 1/\alpha$ which, for $\alpha \ll 1$, is more constraining than the usual semiclassical requirement of slow variation of the de Broglie wave length with position $|dn^{-1/2}/dr| \ll 1$ [7].

A. Potential and density profiles in large distance limit

Even though Eqs. (27) and (28) appear to be good starting points of analysis in the weak, $Z\alpha^2 \ll 1$, and strong, $Z\alpha^2 \gg 1$, screening limits, respectively, below we are going to find out that such treatments inevitably break down at sufficiently large distance from the source center. So we begin with analysis of this large-distance regime by employing the differential equation (16) approximating full integral equations such as (22) or (23). Combining Eq. (16) (with n_{ext} neglected) and Eq. (21), and employing the screening function $\zeta(r)$ introduced in Eq. (18) we arrive at the nonlinear differential equation

$$\zeta''(l) - \zeta'(l) = 2\alpha^2 \zeta^2 \tag{31}$$

whose immediate consequence is that $\zeta \propto \mathcal{Z} \propto 1/\alpha^2$. For $l = \ln(r/R) \ll 1$ [R is now a scale beyond which n_{ext} in Eq. (16) can be omitted compared to n], we can neglect here the first-order derivative term $\zeta'(l)$ compared to $\zeta''(l)$. The solution to (31) in this limit as well as the expression for the net charge within a circle of radius $r = Re^l$, $\mathcal{Z}(l) = -\zeta'(l)$ [see Eq. (19)] are given by

$$\zeta(l) = \frac{3}{\alpha^2(l + B)^2}, \quad \mathcal{Z}(l) = \frac{6}{\alpha^2(l + B)^3}, \, 0 \leqslant l \ll 1. \tag{32}$$

Even though Eq. (31) does not mention the source charge distribution, its imprints may be present in the length scale R and value of the numerical constant B determined by matching (32) to its $r \lesssim R$ counterpart (see below).

For $l = \ln(r/R) \gg 1$, we can neglect in Eq. (31) the second-order derivative term $\zeta''(l)$ compared to $\zeta'(l)$. In this limit we do not distinguish between the charge $\mathcal{Z}$ and screening function ζ and can write down Eq. (31) as the equation for the charge

$$\mathcal{Z}'(l) = -2\alpha^2 \mathcal{Z}^2(l). \tag{33}$$

Its solution

$$\mathcal{Z} = \zeta = \frac{1}{2\alpha^2 l} = \frac{1}{2\alpha^2 \ln(r/R)}, \, 1 \ll \ln \frac{r}{R} \ll \frac{1}{\alpha} \tag{34}$$

(with R identified with a lattice length scale) was given previously [10], while the range of applicability (the charge $\mathcal{Z}$ should significantly exceed $1/\alpha$) imposes the constraint $\alpha \ll 1$ [11]. Suspended graphene, $\alpha \approx 1/2$ [4], is at best at the verge of applicability of the asymptotic result; the range in (34) can be made wider by choosing smaller α which can be accomplished by selecting large κ substrates [11]. The potential $\varphi(r) = \zeta(r)e/\kappa r$ and density (21) in this regime are given by

$$\varphi(r) = \frac{e}{2\alpha^2 \kappa r \ln(r/R)}, \tag{35}$$

$$n(r) = \frac{1}{4\pi \alpha^2 r^2 \ln^2(r/R)}. \tag{36}$$

The remarkable property of Eqs. (34)–(36) is their near universality: the dependence on external charge distribution is logarithmically weak and hidden in the length scale R yet to be identified.

B. Weak screening: $Z\alpha^2 \ll 1$

The condition of weak screening is consistent with the source charge being supercritical $Z\alpha \gg 1$ provided $1/\alpha \ll Z \ll 1/\alpha^2$, which almost certainly leaves suspended graphene, $\alpha \approx 1/2$ [4], outside of this regime [11]. For graphene on a high-κ substrate ($\alpha \ll 1$), the weak-screening regime can be realized and the starting point of the analysis is the zero-screening limit result (10). Then substitution of $\varphi = \varphi_{\text{ext}}$ into Eq. (21) determines the electron density as the effect of the order $Z\alpha^2$ [see Eq.(26)]:

$$n(r) = \frac{1}{\pi}\left(\frac{e\varphi_{\text{ext}}(r)}{\hbar v_F}\right)^2 \rightarrow \frac{Z^2\alpha^2}{\pi r^2}, \qquad (37)$$

where in the second step we specified to the $r \gg a$ limit. Inside the source charge distribution, the density can be estimated as $n(r \lesssim a) \simeq Z^2\alpha^2/a^2$, and the number of screening electrons is of the order $(Z^2\alpha^2/a^2)a^2 = Z \cdot (Z\alpha^2) \ll Z$. We thus conclude that most of the screening charge is outside the source charge distribution. For the total charge within a circle of radius $r \gg a$ we find with logarithmic accuracy

$$\mathcal{Z}(r) = Z - 2\pi \int_0^r n(r')r'dr' = Z\left(1 - 2Z\alpha^2 \ln\frac{r}{a}\right), \quad (38)$$

which applies provided $Z\alpha^2 \ln(r/a) \ll 1$, i.e., it inevitably fails at sufficiently large distance from the source [the density (37) is not normalizable].

Equations (38) and (34) (with $R \to a$) can be combined into a compact interpolation formula that captures both perturbative short-distance and nearly universal large-distance limits, respectively,

$$\mathcal{Z}(r) \simeq \frac{Z}{1 + 2Z\alpha^2 \ln(r/a)}, \quad 1 \lesssim \ln\frac{r}{a} \ll \frac{1}{\alpha}, Z\alpha^2 \ll 1 \tag{39}$$

[and ignores the intermediate asymptotic regime (32)]. The same accuracy interpolation formula can be given for the electron density

$$n(r) \simeq \frac{Z^2\alpha^2}{\pi r^2[1 + 2Z\alpha^2 \ln(r/a)]^2} \qquad (40)$$

that combines Eqs. (36) and (37). It is straightforward to verify that (with accuracy controlled by the $Z\alpha^2 \ll 1$ condition) the density distribution (40) is normalized at Z, and that the net charge within a circle of radius $r \gtrsim a$ computed with the help of Eq. (40) reproduces Eq. (39).

Finally, the interpolation formula for the potential

$$\varphi(r) \simeq \frac{Ze}{\kappa r[1 + 2Z\alpha^2 \ln(r/a)]} \qquad (41)$$

follows from the relationship (21). While Eqs. (39)–(41) were given previously [10], their status as interpolation formulas was not clarified; their range of applicability as given in Eq. (39) was pointed out in Ref. [11].

C. Strong screening: $Z\alpha^2 \gg 1$

The starting point of the analysis is the classical result (11). Then substitution of $n = n_{\text{ext}}$ into Eq. (21) determines the potential as the effect of the order $(Z\alpha^2)^{-1/2}$ [see Eq. (26)]. This is an improvement on Eq. (11) to the case of large finite screening parameter $Z\alpha^2$:

$$n(r) = n_{\text{ext}}(r), \quad \varphi(r) = \frac{\hbar v_F \sqrt{\pi n_{\text{ext}}(r)}}{e}, \quad r \ll R. \quad (42)$$

The length scale R limiting the range of applicability can be determined by recalling that in the strong screening limit, the kinetic energy of the confined electrons having quantum-mechanical origin is negligible compared to the classical potential energy of the Coulomb repulsion. Comparing the first and third term of the energy functional (24), it is straightforward to realize that they have the same order of magnitude at the scale R to be self-consistently determined from the condition,

$$R \simeq \frac{1}{\alpha\sqrt{n_{\text{ext}}(R)}}. \qquad (43)$$

We note the right-hand side has the same order of magnitude as the screening length [18] of the two-dimensional electron gas $(\kappa/2\pi e^2)\partial\mu_0/\partial n$ of density n_{ext}, which in graphene's case is $1/4\alpha\sqrt{\pi n_{\text{ext}}}$. It is a consequence of dimensional analysis applied to Eq. (43) that the electron charge outside the $r \simeq R$ circle can be estimated as $n(R)R^2 \simeq 1/\alpha^2$ which is also an estimate for the *net* charge inside the $r \simeq R$ circle, i.e., $\mathcal{Z}(R) \simeq 1/\alpha^2$ (total electric charge of the source plus that of the electron cloud is zero in the TF theory). Earlier (Sec. III A), R was defined as a length scale beyond which n_{ext} can be neglected compared to n. However, in that regime the charge was also found to be proportional to $1/\alpha^2$. Specifically, $l = 0$ in the equation for the charge (32) means $r = R$, thus implying that $\mathcal{Z}(R) \simeq 1/\alpha^2 B^3$. It then seems plausible that at $r \simeq R$, determined by Eq. (43), the density and potential given by Eq. (42) cross over to their $r \gtrsim R$ counterparts as described in Sec. III A, and that the coefficient B in Eq. (32) is a Z-independent constant.

As evidenced by Eq. (28), relative correction to $n = n_{\text{ext}}$ has the order of $(Z\alpha^2)^{-1/2}$ and thus is small for $r \ll R$. Explicit calculation for the charge off the plane geometry [11] illustrates this assessment.

For suspended graphene, $\alpha \approx 1/2$ [4], $Z \gg 1$, and sufficiently smooth n_{ext} properties of the bulk of the electron screening cloud, $r \lesssim R$, are described by Eqs. (42) and (43). For the special case of the external point charge positioned off the graphene plane, this conclusion was reached in Ref. [11]. Properties of the cloud fringe, $r \gtrsim R$, may be captured semi-quantitatively by the theory of Sec. III A.

1. External point charge off graphene plane

For the special case of point, external charge Z positioned a distance a away, the graphene plane the results (42) and (43) were derived earlier [11]. The length scale (43) in this case can be estimated as $R \simeq a \cdot (Z\alpha^2) \gg a$ and direct integration of the density (7) verifies our dimensional argument that the net charge within a circle of radius R, $\mathcal{Z}(R) = Z - 2\pi \int_0^R n_{\text{ext}}(r)rdr$, is indeed of the order $1/\alpha^2$. It was stated

[11] that the conclusions

$$n(r) = \frac{Za}{2\pi r^3}, \quad \varphi(r) = \frac{\hbar v_F}{e}\sqrt{\frac{Za}{2r^3}}, \quad a \ll r \ll a \cdot (Z\alpha^2)$$

(44)

originally derived for the charge off the plane geometry, specifically the power-law falloffs $n(r) \propto 1/r^3$ and $\varphi(r) \propto 1/r^{3/2}$ within specified range of distances (44), are universally applicable for generic external charge distribution of net charge Z spread over a length scale a. We disagree and give two experimentally relevant examples of external in-plane charge distributions.

2. Gaussian external charge distribution

If the external charge distribution is Gaussian, Eqs. (8), (42), and (43) now predict that

$$n(r) = \frac{Z}{4\pi a^2}e^{-r^2/4a^2},$$

$$\varphi(r) = \frac{\hbar v_F \sqrt{Z}}{2ea}e^{-r^2/8a^2}, \quad r \ll R \simeq 2a\ln^{1/2}(Z\alpha^2). \quad (45)$$

We see that for Gaussian distribution of external charge the potential is also Gaussian and drastically different from the external potential (9). The expression for the length scale R has logarithmic accuracy and exhibits weak dependence on the screening parameter $Z\alpha^2$. In practical terms the latter means that the potential is present where the external charge is.

3. Uniformly charged disk: Realization of two-dimensional Thomson atom

Vacancy clusters in graphene, if created by the technique of Ref. [6], would have atomically sharp boundaries. The relevant external charge distribution is then that of an in-plane uniformly charged disk of radius a. Then, within the cluster, the electron density and potential are constant and given by Eq. (42) (the state of local neutrality), and zero otherwise. This solution predicts singularity of the in-plane electric field at the boundary which is removed for large but finite screening parameter $Z\alpha^2$. Indeed, quantum mechanics (finite $Z\alpha^2$) promote delocalization and as a result some fraction of the screening electrons move outside of the geometrical boundary of the cluster while the majority remains inside. As in analogous problem of impurity screening in Weyl semimetals [13], the concept of the screening length (43) (with constant n_{ext}) continues to play an important role and gives an estimate of the width of the charge depleted region within the cluster. Only within this layer is the external charge not locally neutralized; a small fraction of screening electrons resides outside the cluster. This physical picture is internally consistent if the size of the depleted region $a/\sqrt{Z\alpha^2}$ is significantly smaller than the cluster size a, which indeed holds in the strong-screening limit $Z\alpha^2 \gg 1$.

This argument allows us to estimate the net charge within the cluster as the external charge within the electron depleted boundary region,

$$\mathcal{Z}(a) \simeq a(Z\alpha^2)^{-1/2} \cdot a \cdot n_{\text{ext}} \simeq Z \cdot (Z\alpha^2)^{-1/2} \ll Z, \quad (46)$$

which is simultaneously the estimate for the number of screening electrons outside the cluster. We see that the majority of

the screening electrons are inside the cluster while only a small fraction is outside where the description of Sec. III A (with $R \simeq a$) applies. Matching the charges given by Eqs. (46) and (32) at the cluster boundary the coefficient B entering Eq. (32) can be estimated as $B \simeq (Z\alpha^2)^{-1/2}$.

The uniformly charged cluster along with the screening cloud of electrons is in itself an interesting object because it provides two-dimensional realization of the Thomson atom, a now obsolete model of real atom. In our case, the "nucleus"—the bulk of the cluster—is nearly perfectly neutralized by the electrons with the exception of positively charged boundary layer while the small fraction of the screening cloud is present outside the cluster. The boundary region forms a two-dimensional electrostatic double layer where the outward-pointing electric field is localized. The near neutrality of the bulk of the cluster is the classical effect while the double-layer structure of the boundary region has quantum-mechanical origin.

IV. CONCLUSIONS

Piecing together the results of analysis of various limiting cases, we arrive at the following physical picture of screening of a highly charged, $Z\alpha \gg 1$, impurity cluster in graphene:

(i) The outcome is largely dictated by the dimensionless screening parameter $Z\alpha^2$ and, to a lesser extent, by the smoothness of the external charge distribution. If $\alpha \ll 1$ (graphene on high-κ substrate), there are two well-defined regimes of parameter values.

(ii) In the weak-screening case, $Z\alpha^2 \ll 1$, most of the screening charge resides outside the cluster; it is nearly certain that this regime cannot be realized in suspended graphene, $\alpha \approx 1/2$.

(iii) In the strong-screening regime, $Z\alpha^2 \gg 1$, most of the screening charge resides inside the cluster, and this regime does apply to the case of suspended graphene. Experimentally, the most relevant situation of a uniformly charged cluster with sharp boundary provides two-dimensional realization of the Thomson atom. As the screening parameter $Z\alpha^2$ is tuned [6] from small to large values, the screening cloud gradually moves inside the cluster interpolating between the regimes of weak and strong screening.

(iv) If $\alpha \ll 1$, the fringe of the screening cloud, regardless of the value of $Z\alpha^2$, exhibits nearly universal properties. For suspended graphene, $\alpha \approx 1/2$, this regime most likely does not exist.

We hope that our results will motivate future experimental efforts to extend the approach of Ref. [6] to vacancy clusters in graphene. These clusters could be gradually charged so that with appropriately chosen substrates the dimensionless screening parameter $Z\alpha^2$ could be tuned from the weak, $Z\alpha^2 \ll 1$, to the strong, $Z\alpha^2 \gg 1$, screening regimes. Graphene's screening response will be monitored, including realization of a two-dimensional Thomson atom in the strong screening regime.

[1] A. H. Castro Neto, F. Guinea, N. M. R. Peres, K. S. Novoselov, and A. K. Geim, The electronic properties of graphene, Rev. Mod. Phys. **81**, 109 (2009); and references therein.

[2] Y. B. Zel'dovich and V. S. Popov, Electronic structure of superheavy atoms, Usp. Fiz. Nauk **105**, 403 (1971) [Sov. Phys. Usp. **14**, 673 (1972)]; V. S. Popov, Critical charge in quantum electrodynamics, Yad. Fiz. **64**, 421 (2001) [Phys. Atom. Nuclei **64**, 367 (2001)]; and references therein.

[3] A. V. Shytov, M. I. Katsnelson, and L. S. Levitov, Vacuum polarization and screening of supercritical impurities in graphene, Phys. Rev. Lett. **99**, 236801 (2007).

[4] J. González, F. Guinea, and M. A. H. Vozmediano, Non-Fermi liquid behavior of electrons in the half-filled honeycomb lattice (A renormalization group approach), Nucl. Phys. B **424**, 595 (1994); F. Guinea, J. González, and M. A. H. Vozmediano, Non fermi liquid behavior in semimetals. Applications to the fullerenes, J. Low Temp. Phys. **99**, 287 (1995).

[5] Y. Wang, D. Wong, A. V. Shytov, V. W. Brar, S. Choi, Q. Wu, H.-Z. Tsai, W. Regan, A. Zettl, R. K. Kawakami, S. G. Louie, L. S. Levitov, and M. F. Crommie, Observing atomic collapse resonances in artificial nuclei on graphene, Science **340**, 734 (2013).

[6] J. Mao, Y. Jiang, D. Moldovan, G. Li, K. Watanabe, T. Taniguchi, M. Ramezani Masir, F. M. Peeters, and E. Y. Andrei, Realization of a tunable artificial atom at a supercritically charged vacancy in graphene, Nat. Phys. **12**, 545 (2016).

[7] L. D. Landau and E. M. Lifshitz, *Quantum Mechanics: Non-Relativistic Theory*, 3rd ed. (Butterworth-Heinemann, 1981), Vol. III, Chaps. 7 and 10.

[8] E. H. Lieb and B. Simon, The Thomas-Fermi theory of atoms, molecules and solids, Adv. Math. **23**, 22 (1977).

[9] D. P. DiVincenzo and E. J. Mele, Self-consistent effective-mass theory for intralayer screening in graphite intercalation compounds, Phys. Rev. B **29**, 1685 (1984).

[10] M. I. Katsnelson, Nonlinear screening of charge impurities in graphene, Phys. Rev. B **74**, 201401(R) (2006).

[11] M. M. Fogler, D. S. Novikov, and B. I. Shklovskii, Screening of a hypercritical charge in graphene, Phys. Rev. B **76**, 233402 (2007).

[12] A. B. Migdal, D. N. Voskresenskî, and V. S. Popov, Distribution of vacuum charge near supercharged nuclei, Pis'ma Zh. Eksp. Teor. Fiz. **24**, 186 (1976) [Sov. Phys. JETP Lett. **24**, 163 (1976)]; A. B. Migdal, V. S. Popov, and D. N. Voskresenskî, The vacuum charge distribution near super-charged nuclei, Zh. Eksp. Teor. Fiz. **72**, 834 (1977 [Sov. Phys. JETP **45**, 436 (1977)].

[13] E. B. Kolomeisky, J. P. Straley, and H. Zaidi, Fermion space charge in narrow band-gap semiconductors, Weyl semimetals, and around highly charged nuclei, Phys. Rev. B **88**, 165428 (2013).

[14] L. V. Keldysh, Low-lying levels in semiconductors, Zh. Eksp. Teor. Fiz. **45**, 364 (1963) [Sov. Phys. JETP **18**, 253 (1964)].

[15] A. A. Abrikosov and S. D. Beneslavskii, Possible existence of substances intermediate between metals and dielectrics, Zh. Eksp. Teor. Fiz. **59**, 1280 (1970) [Sov. Phys. JETP **32**, 699 (1971)]; Some properties of gapless semiconductors of the second kind, J. Low Temp. Phys. **5**, 141 (1971).

[16] H. Fu, K. V. Reich, and B. I. Shklovskii, Collapse of electrons to a donor cluster in $SrTiO_3$, Phys. Rev. B **92**, 035204 (2015).

[17] I. S. Gradshteyn and I. M. Ryzhik, *Table of Integrals, Series and Products*, 5th ed. (Academic, New York, 1994), p. 732, 6.618.1, p. 912, 8.126.3 (Landen's transformation).

[18] T. Ando, A. B. Fowler, and F. Stern, Electronic properties of two-dimensional systems, Rev. Mod. Phys. **54**, 437 (1982); and references therein.